Chaos, Solitons and Fractals 104 (2017) 198–208

Contents lists available at ScienceDirect

Chaos, Solitons and Fractals

Nonlinear Science, and Nonequilibrium and Complex Phenomena

journal homepage: www.elsevier.com/locate/chaos

The effect of high viscosity on the evolution of the bifurcation set of a periodically excited gas bubble

Kálmán Klapcsik*, Ferenc Hegedűs

Department of Hydrodynamic Systems, Faculty of Mechanical Engineering, Budapest University of Technology and Economics, Budapest, P.o. Box 91. 1521, Hungary

ARTICLE INFO

Article history:
Received 31 May 2016
Revised 1 August 2017
Accepted 22 August 2017

Keywords:
Bubble dynamics
Bifurcation structure
Dissipation mechanism
Keller–Miksis equation
Bi-parametric maps
Farey-tree
GPU accelerated IVPs

ABSTRACT

In this study, a nonlinear investigation of a periodically driven gas bubble in glycerine is presented. The bifurcation structure of the bubble oscillator (Keller–Miksis equation) is explored in the pressure amplitude-frequency parameter plane of the excitation by means of initial (high resolution bi-parametric plots) and boundary value problem solvers at various ambient temperatures. The range of the applied temperature covers two orders of magnitude difference in the liquid viscosity which is the main damping factor of the system. Therefore, the evolution of the harmonic and ultraharmonic resonances are presented starting with an overdamped behaviour (there are no resonances in the parameter space) and ending up with a fully developed bifurcation superstructure. The results reveal a complex period bubbling mechanism organized in a Farey-tree; inside each bubble a fine substructure of alternating chaotic and periodic bands exist. The description of the bifurcation structure presented throughout the paper can help to understand the mechanism of dissipation on the behaviour of nonlinear systems in more detail.

1. Introduction

The interaction of high intensity and high frequency sound waves with liquid domains can lead to the phenomenon called acoustic cavitation, which produces bubble clusters. These are usually composed by micron-sized gas bubbles oscillating around their equilibrium size. When the intensity reaches Blake's threshold [1], the bubbles become cavitationally active, and start to oscillate with high amplitude. During the radial oscillation of such bubbles, at the minimum bubble radius (collapse phase), the temperature and pressure in the bubble interior can exceed thousands of Kelvin and bar, respectively [2]. Cavitationally active bubbles always grow by rectified diffusion [3–6] due to the much larger diffusive area at the expansion phase than at the collapse phase. The limit of the growth is the size where the bubble lose its spherical stability [7,8]. Spherically unstable bubbles disintegrate into smaller bubbles, which start to grow again by rectified diffusion, or dissolve into the liquid domain. This process is called bubble life cycle, for the details see [9–11].

The time scale of the life cycle of a bubble is greater by many orders of magnitude than the period of its radial oscillation. Therefore, it is reasonable to investigate a single individual bubble as a building block of clusters. The dynamics of such bubbles shows highly nonlinear properties. Modern numerical techniques and methods of chaos physics revealed the existence of harmonic and subharmonic resonances in the pressure amplitude-frequency plane [12–19], the presence of period-doubling route to chaos [20–25] and the alteration of chaotic and periodic windows [26–29] in the bifurcation pattern. The majority of these nonlinear features have already been proven experimentally. Subharmonics in the spectrum of the response of a bubble was observed first by Esche [30]. Later, Lauterborn and his co-workers successfully justified the existence of period-doubling route to chaos in water [31,32]. Chaotic bubble oscillation was also found by high-speed holographic cinematography [33], and by measuring the time delays between flashes of emitted light (sonoluminescence [34–36]) at the collapse phase of a bubble [37].

The aforementioned knowledge accumulated over decades in nonlinear bubble dynamics is usually related to water (few exceptions are [38–41]). Therefore, the present study intends to investigate a gas bubble in glycerine with varying temperature (between 20 °C and 70 °C); that is, the viscosity is varied between two orders of magnitude (see Table C.2) leading to three to one orders of magnitude higher values than of water. It is well-known that high viscosity causes huge damping effect [42,43], which implies a much less feature-rich bubble dynamics. Throughout this paper, the evolution of the bifurcation structure in the pressure amplitude-frequency plane with decreasing damping factor is ex-

* Corresponding author.
E-mail addresses: kklapcsik@hds.bme.hu (K. Klapcsik), fhegedus@hds.bme.hu (F. Hegedűs).

http://dx.doi.org/10.1016/j.chaos.2017.08.022
0960-0779/

amined and compared with results obtained on other nonlinear oscillators such as Toda [44], Duffing [45–47], Morse [48] and bubbles in water (see the discussion above).

The applied bubble model is the Keller–Miksis equation, which is a second order ordinary nonlinear differential equation that takes into account the compressibility of the liquid to the first order. The numerical tools are an initial value problem solver (shooting method implemented in CUDA C to exploit the high numerical computing power of GPUs) and a boundary value problem solver combined with the pseudo-arch length continuation technique (AUTO). These advanced numerical techniques of nonlinear science provide a better insight into the highly damped bubble oscillations than the previous studies, see e.g. [43].

2. Mathematical model

The employed bubble model is the same as in our previous paper [26], thus here, it is summarized briefly. The modified form [22] of the Keller–Miksis equation [49], which describes the evolution of the bubble radius $R(t)$ in time is

$$\left(1-\frac{\dot{R}}{c_L}\right)R\ddot{R}+\left(1-\frac{\dot{R}}{3c_L}\right)\frac{3}{2}\dot{R}^2=\left(1+\frac{\dot{R}}{c_L}+\frac{R}{c_L}\frac{d}{dt}\right)\frac{(p_L-p_\infty)}{\rho_L}, \tag{1}$$

where c_L is the sound velocity in the liquid, ρ_L is the density of the liquid, and the dot stands for the derivative with respect to time. The pressure far away from the bubble

$$p_\infty(t)=P_\infty+p_A\sin(\omega t) \tag{2}$$

consist of a static and a periodic component, where P_∞ is the ambient pressure, p_A is the pressure amplitude and ω is the angular frequency of the excitation.

The pressure inside the bubble is the sum of the partial pressures of the non-condensable gas p_G and vapour p_V. The liquid pressure at the bubble wall is p_L. The three kinds of pressures are connected by the dynamic mechanical equilibrium at the interface:

$$p_G+p_V=p_L+\frac{2\sigma}{R}+4\mu_L\frac{\dot{R}}{R}, \tag{3}$$

where σ is the surface tension and μ_L is the liquid dynamic viscosity.

The gas content obeys a simple polytropic state of change

$$p_G=p_{G0}\left(\frac{R_0}{R}\right)^{3n}, \tag{4}$$

where R_0 and p_{G0} are the reference radius and pressure, respectively. The polytropic exponent is $n=1.4$ assuming adiabatic gas behaviour.

2.1. Parameters and material properties

During the computations, the ambient pressure $P_\infty=1$ bar was constant. The ambient temperature T_∞, which is one of the control parameter, specifies all the liquid material properties (the pressure dependence can be negligible), which were determined by means of the experiments of the Dow Chemical Company. The tabulated values are summarized in Appendix C.

The bubble size is given by the equilibrium radius $R_E=0.1$ mm of the unexcited system ($p_A=0$). This is a common way to prescribe the size of the bubble. Now, if the reference radius is set to $R_0=R_E$ then the gas reference pressure can be expressed as

$$p_{G0}=\frac{2\sigma}{R_E}-(p_V-P_\infty). \tag{5}$$

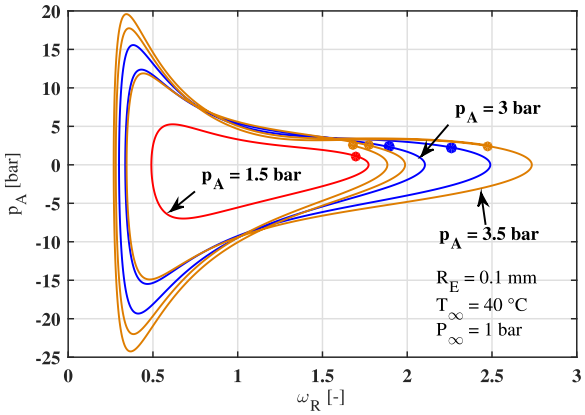

Fig. 1. Examples of period 1 (red), 2 (blue) and 3 (orange) attractors in the dimensionless phase plane at pressure amplitudes 1.5, 3 and 3.5 bar, respectively. The dots denote the points of the Poincaré section. (For interpretation of the references to colour in this figure legend, the reader is referred to the web version of this article.)

The two remaining parameters are related to the acoustic irradiation, namely, the pressure amplitude p_A and the angular frequency ω. The angular frequency is normalized with the undamped linear eigenfrequency [2]

$$\omega_E=\sqrt{\frac{3n(P_\infty-p_V)}{\rho_L R_E^2}+\frac{2(3n-1)\sigma}{\rho_L R_E^3}} \tag{6}$$

of the system, which defines the relative frequency as

$$\omega_R=\frac{\omega}{\omega_E}. \tag{7}$$

During the computations, dimensionless variables were used: dimensionless bubble radius $x_1=R/R_E$, dimensionless time $\tau=t/(2\pi/\omega)$ and dimensionless bubble wall velocity $x_2=x_1'$, where the $'$ stands for the derivative with respect to τ. The dimensionless equation system is given in Appendix A.1 in detail.

3. Numerical tools

3.1. Initial value problem solver and Poincaré section

Due to the strong nonlinearity of the Keller–Miksis equation, analytical solutions are not known to be exist, but numerical solutions can be easily obtained. The simplest method is to use an initial value problem (IVP) solver with suitable initial conditions and integrate the system forward in time. After several acoustic cycles, the transient trajectory converges to a stable solution called attractor. Since the bubble is periodically excited, the simplest solution is a closed periodic orbit. If the converged trajectory repeats itself after m acoustic cycles, it is called period m orbit. Fig. 1 shows different periodic attractors in the dimensionless x_1-x_2 phase plane. The red, blue and orange curves show period 1, 2 and 3 solutions calculated at pressure amplitudes 1.5, 3 and 3.5 bar, respectively.

As one can see from Fig. 1, the trajectories of the periodic solutions can intersect themselves and each other in the phase plane producing overcrowded figures. To avoid this difficulty, only some characteristic properties of the solutions were recorded such as the periodicity or the points of the Poincaré map obtained by sampling the continuous trajectory at the end of every acoustic period. The points of the Poincaré section of the periodic orbits in Fig. 1 are denoted by the dots. The period of the bubble oscillation may even tends to infinity never repeating itself. This type of solution called chaotic attractor. An example is given in Fig. 2 by its 10,000 number of Poincaré points.